JOURNAL OF VIROLOGY, June 2005, p. 6644–6654 Vol. 79, No. 11
0022-538X/05/$08.00+0 doi:10.1128/JVI.79.11.6644–6654.2005

Influenza Type A Virus Escape Mutants Emerge In Vivo in the Presence of Antibodies to the Ectodomain of Matrix Protein 2

Darya Zharikova, Krystyna Mozdzanowska, Jingqi Feng, Manxin Zhang, and Walter Gerhard*

The Wistar Institute, 3601 Spruce Street, Philadelphia, Pennsylvania 19104-4268

Received 17 November 2004/Accepted 24 January 2005

The ectodomain of matrix protein 2 (M2e) of human influenza type A virus strains has remained remarkably conserved since 1918. Because M2e-specific immunity has been shown to decrease morbidity and mortality associated with influenza virus infection in several animal models and because natural infection and current vaccines do not appear to induce a good M2e-specific antibody (Ab) response, M2e has been considered as potential vaccine for inducing cross-reactive protection against influenza type A viruses. The high degree of structural conservation of M2e could in part be the consequence of a poor M2e-specific Ab response and thus the absence of pressure for change. To assess this possibility, we studied the course of infection in SCID mice in the presence or absence of passive M2e-specific monoclonal Abs (MAbs). We found that virus mutants with antigenic changes in M2e emerged in 65% of virus-infected mice treated with M2e-specific but not control MAbs. However, the diversity of escape mutants was highly restricted since only two types were isolated from 22 mice, one with a proline-to-leucine and the other with a proline-to-histidine interchange at amino acid position 10 of M2e. The implications of these findings for the use of M2e as a broadly protective vaccine are discussed.

Current influenza virus vaccines aim to induce strong antibody (Ab) responses to the ectodomains of hemagglutinin (HA) and neuraminidase (NA) molecules, since these antibodies (Abs) can provide potent protection against infection and/or disease. The main deficiency of this protection is that it targets highly variable viral determinants. This necessitates not only frequent updating of the vaccine to contemporary circulating virus strains but, given that vaccines have to be produced and applied ahead of exposure to epidemic strains, also a correct prediction of these future epidemic strains. Failure to anticipate the emergence of an epidemic strain with significant antigenic changes compared to the vaccine strain will greatly reduce vaccine-induced protection. It would be advantageous, therefore, to expand vaccine-mediated protection to less variable viral targets. One possible way to achieve this may be through induction of M2e-specific Abs (6, 9, 10, 14, 18, 21, 24, 28).

M2 is a 97-amino-acid transmembrane protein of influenza type A virus (15, 16). The mature protein forms homotetramers (12, 29) that have pH-inducible ion channel activity (27, 29). M2-tetramers are expressed at high density in the plasma membrane of infected cells but are relatively excluded from sites of virus maturation and therefore incorporated only at low frequency into the membrane of mature virus particles (30, 33). Most important in the present context are, first, that the sequence of the 24-amino-acid ectodomain of M2 (M2e) has remained remarkably conserved among human epidemic virus strains (Fig. 1A) (20). Indeed, the majority of human epidemic strains isolated since 1918 share the same M2e protein sequence. Second, several studies in mice have shown that M2e-specific Abs restrict influenza virus replication and reduce morbidity and mortality (6, 19, 23, 24, 31). Furthermore, a recent study in ferrets, the animal model considered most prognostic for human influenza, has demonstrated protective activity of M2e-specific immunity (6), and sera from rhesus monkeys immunized with a M2e-carrier conjugate have been shown to exhibit protective activity upon transfer into mice (6). Thus, with the exception of a recent study in pigs, which indicated that M2e-specific immunity may enhance rather than ameliorate disease (10), evidence from animal models shows that M2e-specific immunity is capable of providing a significant level of protection that is directed against a remarkably conserved viral target.

The low degree of structural variation in M2e is certainly in part attributable to constraints resulting from its genetic relation to M1, the most conserved protein of the virus (13). M2 is encoded by a spliced RNA of the viral gene segment 7, which codes also for M1 (15). The splicing removes most of the nucleotides that code for M1 (nucleotides [nt] 27 to 714) except the 26 most 5′ and 42 most 3′ nucleotides (15). Thus, nt 1 to 68 of M2, which encode essentially the entire M2e, are bicistronic, from nt 1 to 26 in the same reading frame and from nt 27 to 68 in a different reading frame. This genetic relation between M2e and M1 can be expected to substantially restrict the degree of variability in M2e. An additional factor that may contribute to the low degree of change seen in M2e among human influenza virus strains could be the absence of M2e-specific Abs and thus pressure for change. A small study of 17 paired human sera obtained during the acute and convalescent phase of natural infection found that M2-specific Abs were absent from acute-phase sera and became detectable by enzyme-linked immunosorbent assay (ELISA) in only six of the convalescents (3). This was in contrast to nucleoprotein-specific Ab titers, which increased in 15 of 17 convalescent-phase

* Corresponding author. Mailing address: The Wistar Institute, 3601 Spruce St., Philadelphia, PA 19104-4268. Phone: (215) 898-3840. Fax: (215) 898-3868. E-mail: gerhard@wistar.upenn.edu.

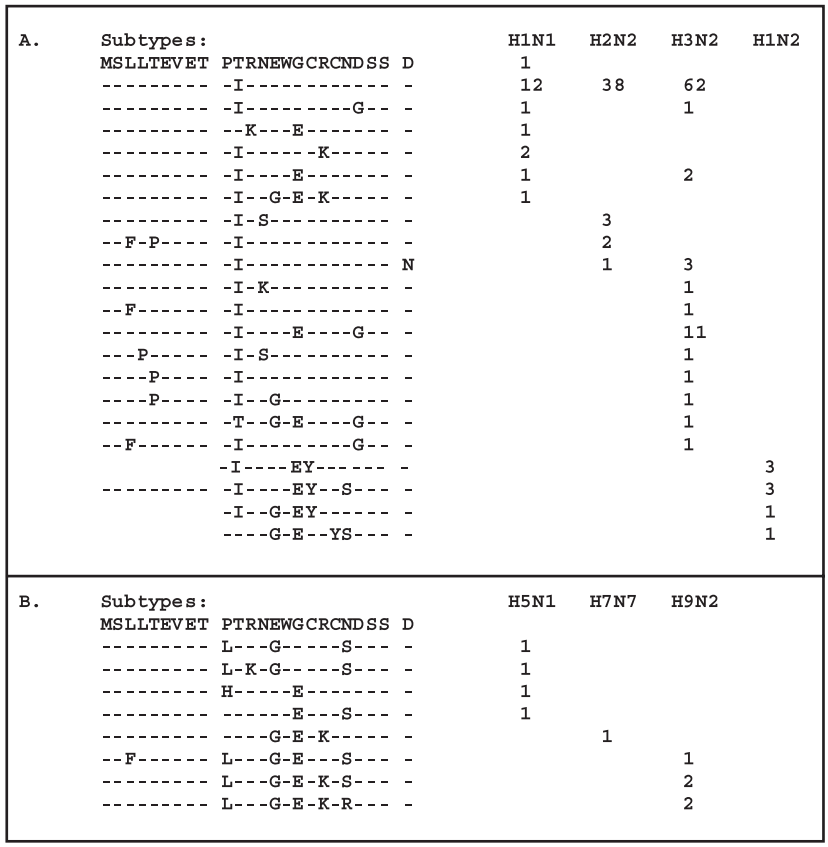

A.	Subtypes:		H1N1	H2N2	H3N2	H1N2
	MSLLTEVET PTRNEWGCRCNDSS	D	1			
	--------- -I----------	-	12	38	62	
	--------- -I---------G--	-	1		1	
	--------- --K---E-------	-	1			
	--------- -I------K-----	-	2			
	--------- -I----E-------	-	1		2	
	--------- -I--G-E-K-----	-	1			
	--------- -I-S----------	-		3		
	--F-P---- -I----------	-		2		
	--------- -I----------	N		1	3	
	--------- -I-K----------	-			1	
	--F------ -I----------	-			1	
	--------- -I----E----G--	-			11	
	---P----- -I-S----------	-			1	
	----P---- -I----------	-			1	
	----P---- -I--G---------	-			1	
	--------- -T--G-E----G--	-			1	
	--F------ -I---------G--	-			1	
	-I----EY------	-				3
	--------- -I----EY--S---	-				3
	-I--G-EY------	-				1
	----G-E--YS---	-				1

B.	Subtypes:		H5N1	H7N7	H9N2
	MSLLTEVET PTRNEWGCRCNDSS	D			
	--------- L---G-----S---	-	1		
	--------- L-K-G-----S---	-	1		
	--------- H-----E-------	-	1		
	--------- ------E---S---	-	1		
	--------- ----G-E-K-----	-		1	
	--F------ L---G-E---S---	-			1
	--------- L---G-E-K-S---	-			2
	--------- L---G-E-K-R---	-			2

FIG. 1. M2e sequence of human influenza type A virus isolates. (A) Human epidemic strains. (B) Sporadic (nonepidemic) isolates believed to have been transmitted to humans directly from infected fowl. The top sequence in each alignment is from the strain A/Brevig Mission/1/1918(H1N1), which caused the "Spanish" flu pandemic of 1918. The M2e sequence is subdivided into three blocks to show the genetic relation between M2e and M1: nt 1 to 26 (codons 1 to 9) and nt 27 to 68 (codons 10 to 23) are bicistronic and encode M2e and M1 in the same or different reading frames, respectively. nt 69 to 72 are monocistronic for M2e. The columns underneath each subtype show the number of epidemic strains (identified in the database by unique geographic location and time of isolation) that exhibit the indicated M2e sequence. Dashes indicate identity to the sequence of A/Brevig Mission/1/1918. No dash indicates sequence data were unavailable. Sequence data are from the Influenza Sequence Database (flu.lanl.gov) (20).

sera, thus confirming recent influenza virus infection of the donors (3). Another study found no difference in M2e-specific Ab titers in two larger groups of unpaired sera, one positive and the other negative for virus-specific Abs (18). These data suggest that, whereas infection in humans can result in a measurable Ab response to M2, the response is not generated consistently and is small and of short duration. Similar observations have been made in the mouse model, where two repetitive infections with virus strains that shared the same M2e induced only low titers of M2e-specific Abs (21). Since M2 is a minor component (<0.5%) of purified virus (33), currently licensed inactivated influenza virus vaccines would not be expected to induce M2e-specific immunity either.

In the present study, we investigated the ability of influenza virus to escape passive M2e-specific MAb-mediated protection in vivo. We used an experimental system in which an initial infection of the nasal epithelium in SCID mice progressed over the course of 2 to 3 weeks to a pulmonary infection. As expected, progression of the disease was significantly delayed in SCID mice treated with M2e-specific MAbs. Unexpectedly, M2e escape mutants arose in 65% of anti-M2e Ab-treated mice. However, the diversity of escape mutants was highly restricted as the same two mutants emerged repetitively in many individual mice. Since a restricted number of M2e variants could easily be incorporated into a vaccine, M2e remains a viable option for broadening protection against influenza type A virus.

MATERIALS AND METHODS

Mice. Female BALB/c mice were purchased from Harlan. C.B17 (SCID) mice were purchased from the Breeding Facility of The Wistar Institute. Mice were maintained in the Institute's Animal Facility under specific-pathogen-free conditions in microisolator cages. All experimental procedures were approved by the Institute's Institutional Animal Care and Use Committee.

Viruses. PR8 [A/PR/8/34/Mt.S/Wi(H1N1)] is a mouse-adapted strain originally obtained from Mt. Sinai Hospital in New York. It differs from the original Mt.S strain by replacement of alanine at position 27 by threonine in the transmembrane domain of M2 (www.flu.lanl.gov). B/Lee is the type B influenza virus strain B/Lee/40. P10, P10H, and P10L are viral isolates from the lungs of three different PR8-infected SCID mice that were chronically treated with the M2e-specific monoclonal Abs (MAbs) M2-80, M2-56, and 14C2-S1-4, respectively. P10 possesses the wild-type (wt) M2 with proline at position 10. P10H and P10L are mutants in which the proline at position 10 is replaced by histidine and leucine, respectively. These three viral isolates were cloned by limiting dilution in MDCK cell microcultures and subsequently grown in 10-day-old embryonated hen's eggs before characterization of their biological properties. Infectious stocks (allantoic fluid containing ca. 10^9 50% tissue culture infective doses [$TCID_{50}$]/ml) were stored frozen at −70°C and used at appropriate dilution for infection.

TABLE 1. Relation between inoculum volume and spread of infection

Vol of inoculum (μl)	Virus titer(s) 2 days p.i. (log_{10})[a]		
	Nose	Trachea	Lung
5	5.07, 4.55	<1.8, <1.8	<2.1, <2.1
10	4.30, 5.01	5.93, 5.39	2.60, 4.69
15	4.14, 4.58	4.58, 3.72	6.31, 5.98
30	4.05, 3.93	4.30, 4.90	6.91, 6.10

[a] PR8 virus at 10^6 $TCID_{50}$/ml of PBS was applied in the indicated volume to the nares (~1/2 of volume/nare) of anesthetized adult female BALB/c mice. Two days later, mice were killed, and nasal turbinates, trachea plus extrapulmonary bronchi, and lungs were collected and tested for virus titer in the MDCK cell assay. Titers (log_{10}, $TCID_{50}$ per total tissue) of two mice per group are shown.

Media and solutions. ISC-CM consists of Iscove Dulbecco medium (Invitrogen) supplemented with 2-mercaptoethanol at 0.05 mM, transferrin (Sigma) at 0.005 mg/ml, L-glutamine at 2 mM (Mediatech-Cellgro), and gentamicin (Mediatech-Cellgro) at 0.05 mg/ml. ISC-CM was further supplemented, as indicated, with fetal calf serum (FCS; HyClone Laboratories) or bovine serum albumin (BSA; Sigma). Hybridoma-SFM is serum-free medium from Invitrogen. PBSN is phosphate-buffered saline (PBS; pH 7.2) containing 3 mM NaN_3.

Antibodies. The M2e-specific MAbs M2-1 M2-15, M2-56, M2-80, and 14C2-S1-4, the nucleoprotein (NP)-specific MAb H16-L10-4R5, and the HA-specific MAb H36-4-5.2 have been described previously (21). They possess κ light and G2a heavy chains. MAR-18.5 (ATCC TIB 216) is a murine hybridoma specific for κ light chain of rat immunoglobulin. MAbs were produced by growth of the corresponding hybridomas in Hybridoma-SFM medium and purified from cell supernatants by adsorption/elution from protein G- or protein A-agarose columns (Pierce). Purified MAbs were then transferred into PBS by filtration/dialysis through collodion membranes (Schleicher & Schuell) or Amicon Ultra filters of 50K exclusion. Ab preparations were sterilized by filtration through a 0.45-μm-pore-size filter membrane (Corning). The Ab concentration was determined by Bio-Rad protein assay and UV light absorption as described previously (7). Ab binding activity was determined in ELISA by titration on plate-bound M2e peptide or fixed monolayers of virus-infected MDCK cells as described previously (21).

Infection, treatment, and analysis of mice. SCID mice (7 to 10 weeks old of either sex) were anesthetized by intraperitoneal injection of 0.2 ml of ketamine-xylazine (70/7 mg/kg) and infected by intranasal (i.n.) administration of 10^3 or 10^4 $TCID_{50}$ of virus in 5 μl of PBS at 2 to 3 μl per nare. This procedure results in an infection that is initially confined to the nasal epithelium. Six to 24 h postinfection (p.i.), antibodies were administered intraperitoneally at 100 μg per mouse. Subsequent antibody injections were given on day 7 and in weekly intervals thereafter at a dose of 50 μg per mouse. These Ab injections resulted in M2e-specific serum Ab titers of 10 to 30 μg/ml, which is in the low range of the active M2e-specific response seen after two immunizations of mice with M2e-MAP (21). Body weight measurements were taken at 1- to 3-day intervals. Severely moribund mice (≥30% loss of the starting body weight) were killed by exsanguination through heart puncture under anesthesia. Nasal turbinates, trachea, and lungs were collected and virus titers determined by titration of tissue extracts in MDCK cell microcultures and/or injection into the allantoic cavity of 10-day-old embryonated hen's eggs as described previously (17). In brief, the respective tissues were harvested aseptically and stored frozen. For virus isolation, frozen tissues were transferred into mortars containing 1 ml (nose and trachea) or 2 ml (lung) of PBS. After the addition of a pinch of sterile carborundum powder, the tissue was ground with a few pestle strokes, the homogenate was transferred to a centrifuge tube, the debris was pelleted, and the supernatant was collected. The latter was then tested for concentration of infectious virus by titration into replicate MDCK cell microcultures (detection threshold of $10^{1.4}$ to $10^{1.8}$ $TCID_{50}$/ml, depending on the starting dilution and number of replicates). Extracts that were negative in the MDCK assay were injected without dilution into the allantoic cavity of embryonated hen's eggs (50 μl/egg, 2 eggs/sample, threshold value of 10 50% egg infective doses/ml). Virus titers relate to the total tissue.

BALB/c mice (female, 9 to 11 weeks old) were infected i.n. under anesthesia with 500 or 1,500 $TCID_{50}$ of PR8 in 50 μl of PBS. This procedure initiates a total respiratory tract infection. Mice were observed for weight loss and mortality.

Antigenic analysis of virus isolates by ELISA. MDCK cells were grown to form confluent monolayers in flat-bottom 96-well Falcon Microtest plates (Becton Dickinson) by seeding wells with 4×10^4 cells in 100 μl of ISC-CM–5% FCS and incubating them overnight at 37°C in 6% CO_2. Monolayers were then washed with PBS to remove serum components and infected by incubation (90 min at 37°C) with 50 μl of individual virus isolates (allantoic fluid from the first egg passage) diluted in ISC-CM–0.1% BSA to give ~10^6 $TCID_{50}$/culture (MOI of ~10). Typically, eight replicate cultures were infected with a given dilution of a virus isolate. After 90 min, 100 μl of ISC-CM–5% FCS was added to each well, and incubation was continued as described above for another 7 to 8 h. Monolayers were then washed with PBSN, fixed by incubation with 5% buffered formalin (Fisher Scientific) for 5 min at room temperature, washed again with PBSN, and blocked and stored with PBSN–1% BSA at 4°C. The infected MDCK cell monolayers were then tested in triplicate (duplicate in case of control) for reaction with M2e-specific, HA-specific, and control (14-4-4S, anti-I-E^k, ATTC HB32) MAbs, each at 1 to 2 μg/ml. Bound MAb was detected by incubation with biotinylated MAb 187 (ATCC HB58, rat anti-mouse-Cκ), and the assay developed by sequential incubation with avidine coupled to alkaline phosphatase and pNPP as described previously (21). The optical density at 405 and 750 nm was measured with the Emax microplate reader (Molecular Devices, Sunnyvale, CA) and the difference ($OD_{405-750}$) was recorded. Mean specific ODs above assay background seen with the control MAb were determined for the anti-HA and anti-M2e MAbs. The OD seen with the anti-M2e MAb was expressed as a percentage of the OD seen with the anti-HA MAb.

Analysis of virus replication in vitro. Portions (50 μl) of virus dilutions (1/3 dilution steps) in ISC-CM–0.1% BSA containing between ca. 10^2 and 10^{-1} $TCID_{50}$ were dispensed into flat-bottom 96-well Microtest plates (Falcon). Freshly trypsinized MDCK cells in ISC-CM–0.1% BSA (4×10^5/ml, 100 μl/well) were added to each well. After incubation of the plates for ~16 h at 37°C to permit adherence of the MDCK cells, trypsin (100 μl, 2 μg/ml ISC-CM–0.1% BSA) was added to each well and incubation at 37°C continued. Starting from 40 h, 15-μl samples of culture medium were collected, and those obtained from replicate cultures at the same time point were pooled. At termination of the experiment after 4 to 5 days of incubation, each individual culture was tested for the presence of virus to determine the infectivity of the virus inoculum and input dose at each dilution step. The virus titer in the pooled samples was determined by HA titration and, if necessary, corrected for the fraction of noninfected cultures at the given dilution. The procedure allowed us to compare the yields of different virus inocula at the same or very similar virus input doses.

Determination of M2 sequence. MDCK or P1.HTR cells were infected with different virus isolates at MOIs of ~20. After 8 to 10 h of infection, total RNA was isolated from cells with TRIzol reagent (Invitrogen). Single-stranded cDNA copies of mRNA were generated with oligo$(dT)_{15}$ primer (Promega) and avian myeloblastosis virus reverse transcriptase (Invitrogen). cDNA template was amplified by PCR with the primer pair M2-3 For (5′-ATGAGTCTTCTAACCGA GGTC-3′), corresponding to genomic nt 26 to 46 (coding region 1 to 21), and M2-4 Rev (5′-CTCCAGCTCTATGCTGAC-3′), corresponding to nucleotide positions 987 to 1004 of M1/M2 cDNA. This generated two PCR products, a 979-bp fragment from nonspliced mRNA encoding both M1 and M2 and a 291-bp fragment from spliced mRNA encoding M2 protein. The fragments were separated by agarose gel electrophoresis, and the M2 fragment was extracted from the gel by using a QIAquick gel extraction kit (Qiagen). To facilitate detection of sequence heterogeneity within viral isolates, the gel-purified 291-bp PCR fragment was directly sequenced by using the M2-1 Rev primer (5′-GAT CCCAATGATATTTGCGGC-3′) that hybridizes to nt 85 to 105 of M2 cDNA and generates an optimal sequence chromatogram through the entire M2e (nt 1 to 72). The 291-bp fragment of 10 isolates was cloned into pCR-TOPO vector (Invitrogen), and both strands of the entire M2 cDNA of two to four clones per isolate were sequenced by using M13 primers. Furthermore, since the first 21 bp of M2 cDNA were primer defined, an additional method was used and applied to selected isolates. In this method, negative-strand viral RNA present in the allantoic fluid was converted into cDNA by using primer M2-2 (5′-GCGAAAG CAGGTAGATATTG-3′), which hybridizes to the 3′ noncoding region of the viral RNA. cDNA was amplified by PCR using M2-2 and SEQ7 (5′-ATATCG TCTCGTATT*AGTAGAAACAAGGTAG*-3′), which is a modified primer described by Hoffmann et al. (11) and anneals to the 5′ noncoding region of vRNA 7 (segment-specific sequence shown in italics). The 1,044-bp PCR product was extracted from the agarose gel with QIAquick kit and sequenced by using primer M2SeqN (5′-CTGTGCGATCTCGGCTTTGAG-3′), which anneals to positions 83 to 103 of M1 cDNA and resolved the first 26 nt of M2 and primer M2SeqC (5′-TCCACAATGTCAAGTGCAAGATC-3′), which hybridizes to positions 815 to 873 of M1 gene and resolved the M2 sequence from positions 27 to 72. This latter method was used for 10 isolates to determine the coding M2 sequence from positions 1 to 21, which was primer defined in the methods described above. All sequences were performed on an ABI 3100 capillary fluorescent sequencer by the Sequence Core Facility of the Wistar Institute. M2 sequences of wt PR8 and

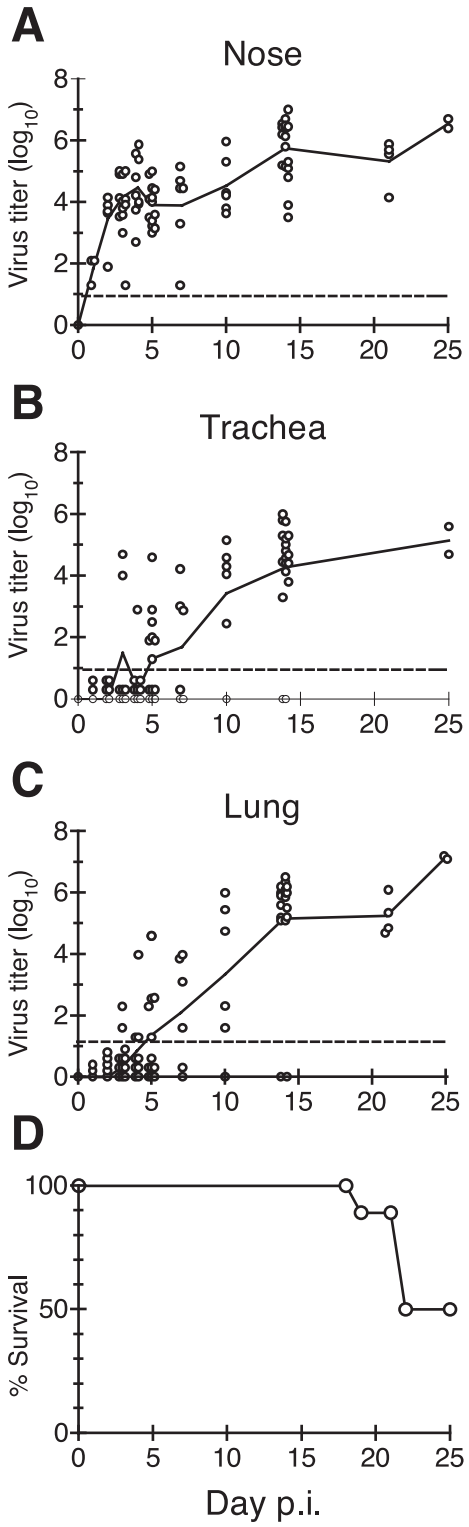

FIG. 2. Progression of a nasal PR8 virus infection in SCID mice. Anesthetized SCID mice were infected i.n. with 5 μl (2 to 3 μl/nare) of PR8 (10^4 $TCID_{50}$). Mice were killed at various times p.i. and tested for the presence of infectious virus in nasal turbinates (A), trachea and extrapulmonary bronchi (B), and lungs (C). Tissue extracts were first titrated in MDCK cell microcultures and, if negative in this assay, injected undiluted (100 μl per two eggs) into the allantoic cavity of 10-day-old embryonated hen's eggs. The stipulated horizontal lines in panels A, B, and C show the threshold of virus detection. Each symbol shows the titer (log_{10}, $TCID_{50}$, or EID_{50} per total tissue) from one mouse. All symbols below the stipulated line indicate absence of detectable infectious virus. The line shows the mean virus titer. All time points except days 1, 21, and 25 p.i. are from two or more independent experiments. (D) Survival. The curve was created by the method of Kaplan and Meier.

escape mutants were submitted to GenBank (accession numbers AY768951 to AY768953).

Statistical analyses. Survival curves were assessed statistically with Prism software, which generates survival curves by the Kaplan-Meier method and compares them for statistical difference by the log-rank test.

RESULTS

Progression of a nasal PR8 virus infection in SCID mice. Unlike HA-specific Abs (22, 25), M2e-specific Abs cannot prevent virus from initiating an infection or resolve an established infection, but they can diminish the yield of infectious virus and thus inhibit progression of the infection (23, 31). We were interested in establishing an experimental system in which the growth-restricting activity of M2e-specific Ab and the capability of influenza virus to escape it could be best assessed in vivo. We reasoned that an experimental system in which the infection progressed from the upper into the lower respiratory tract would be most suitable for this purpose. To establish this model, we first determined the volume of inoculum for initiating an infection that was confined to the nasal epithelium. As shown in Table 1, application of 5 μl (2 to 3 μl/nare) of virus inoculum to anesthetized young adult BALB/c mice resulted in infection of the nasal but not tracheal or pulmonary epithelia, whereas the infection extended into the lower respiratory tract after administration of ≥ 10 μl of inoculum.

Using an inoculum size of 5 μl, we next determined the progression of the nasal PR8 virus infection in SCID mice. In all mice, the infection remained confined to the nasal epithelium for the first 2 days (Fig. 2A) and then began to spread into the lower respiratory tract over the next 10 to 14 days, typically at the same time to both trachea and lung (Fig. 2B and C). In the third and fouth weeks, all SCID mice showed evidence of pulmonary infection and started to die (Fig. 2D). The slow progression of this infection model in SCID mice may be a peculiarity of PR8 or possibly of H1N1 virus strains, since a nasal infection of BALB/c mice with the H3N2 reassortant virus X31 resulted in all mice in a pulmonary infection within 4 days p.i. (data not shown). The slow progression of the nasal PR8 infection in SCID mice provided a suitable system for testing the protective activity of passive M2e-specific MAb in vivo and the capability of the virus to escape it.

Chronic treatment of nasally infected SCID mice with anti-M2e MAbs delayed progression of the infection and resulted in the emergence of M2e-escape mutants. SCID mice were infected i.n. with 5 μl of PR8, treated chronically with M2e-specific or control (NP- or rat-Cκ-specific) MAbs, and monitored for weight loss and mortality. In most cases, mice were euthanized when they had lost >30% of their initial body weight and were severely moribund. This was done to avoid postmortem alterations and bacterial contamination of tissues used for virus isolation.

Figure 3A combines the data of three independent experi-

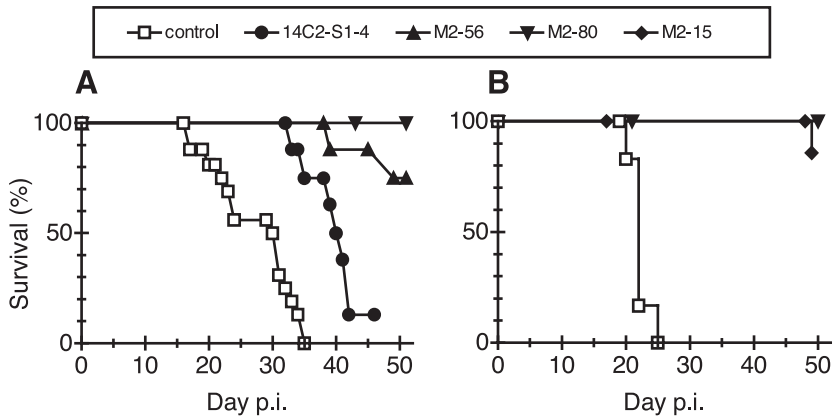

FIG. 3. Chronic treatment of infected SCID mice with M2e-specific MAb prolongs survival. SCID mice were infected i.n. with a 5-μl inoculum containing 10^4 $TCID_{50}$ (A) or 10^3 $TCID_{50}$ (B) of PR8. At 4 to 24 h p.i., mice were injected with 100 μg and at weekly intervals thereafter with 50 μg of purified MAbs specific for NP (□) or M2e: 14C2-S1-4 (●), M2-56 (▲), M2-80 (▼), or M2-15 (◆). Mice were monitored for weight loss and killed when they were severely moribund and had lost ≥30% of their initial body weight, which is defined as survival endpoint. Panel A is a compilation of data from three independent experiments, comprising 16 mice (three experiments) in the control group, 8 mice (one experiment) in the 14C2-S1-4, 8 mice (two experiments) in the M2-56, and 5 mice (one experiment) in the M2-80 group. Panel B shows a single experiment with six mice in the control group and seven mice in each of the anti-M2e MAb treatment groups. In this experiment, the last Ab injection was given on day 42. Experiments were terminated 46 to 56 days p.i. All M2e-specific MAbs significantly increased survival compared to the control group (log rank test, $P < 0.01$).

ments, in which SCID mice were infected with 10^4 $TCID_{50}$ of PR8 and then chronically treated with the M2e-specific MAbs 14C2-S1-4, M2-56, or M2-80 or the NP-specific control MAb H16-L10. All MAbs were used at the same dosage (see legend), which we estimate resulted in a sustained serum MAb concentration of 10 to 30 μg/ml and corresponds to the low range of M2e-specific Ab titers seen in BALB/c mice after two immunizations with M2e-MAP (21). Compared to control MAb, treatment with each of the M2e-specific MAbs significantly prolonged survival of the SCID mice by ~10 days in the case of 14C2-S1-4 and by >20 days in the case of M2-56 and M2-80. Similar findings were made in a fourth experiment (Fig. 3B), in which SCID mice were infected with 10^3 instead of 10^4 $TCID_{50}$ of PR8 and treatment with M2e-specific MAbs M2-80 and M2-15 prolonged survival by >30 days compared to control MAb. The results clearly show that physiologic concentrations of passive M2e-specific MAbs substantially delayed progression of the disease and mortality. In addition, they suggest differences in protective activity between M2e-specific MAbs. The latter finding is rather surprising since all four M2e-specific MAbs are of G2a/κ isotype and recognize an epitope that is contained within the N-terminal 15 amino acids of M2e (our unpublished observation). The underlying reason for these differences remains to be identified.

To determine the concentration of infectious virus in the respiratory tract of infected SCID mice, nasal turbinates, trachea, and lung extracts were titrated for virus by the MDCK assay. All NP- and M2e Ab-treated mice contained a high virus load in the nose and lungs, which was readily detectable by the MDCK assay and ranged from 10^5 to 10^8 $TCID_{50}$/ml of extract (data not shown).

To test for the presence of escape mutants, virus isolates from lungs were propagated once in embryonated hen's eggs, and allantoic fluid was used to infect MDCK cell monolayers in flat-bottom 96-well microtiter plates. The latter were then fixed after 7 to 8 h of incubation and tested by ELISA for recognition by an anti-HA MAb (to measure the degree of infection and provide a positive control) and the anti-M2e MAbs used for treatment of the SCID mice. An example of this assay, in which the M2e-specific Ab binding is expressed as a fraction of HA-specific Ab binding, is shown in Fig. 4. MDCK cells infected with lung isolates from anti-NP and anti-rat-Cκ MAb-treated control mice showed a similar ratio of anti-M2e/anti-HA binding as MDCK cells infected with wt PR8. In contrast, MDCK cells infected with some of the lung isolates from anti-M2e MAb-treated mice showed substantially reduced recognition by M2e-specific MAb (Fig. 4, isolates A8246 to A8259), suggesting that some of the isolates contained M2e-escape mutants. Similar findings were made with lung isolates from all anti-M2e MAb-treated mice. Note that the ELISA may not be effective in detecting mutants in isolates that contain a sizeable proportion of wt virus, since the presence of virus with Ab-reactive wt M2e tends to obscure the presence of nonreactive M2e-escape mutants.

Taken together, the results from Fig. 3 and 4 showed that passive M2e-specific MAbs significantly delayed progression of the nasal infection in vivo and suggested that PR8 virus may be capable of escaping the full protective effect of M2e-specific Abs by antigenic alteration of M2e.

Sequence analysis of virus isolates. The M2 sequence of viral isolates was determined as described in Materials and Methods. Purified PCR products rather than cloned PCR fragments were sequenced in order to facilitate detection of heterogeneity within individual viral isolates. Two types of mutant M2e sequences were observed among the viral isolates from 34 anti-M2e MAb-treated mice; one with a G-to-T interchange and the other with a G-to-A interchange at nucleotide position 29 of M2. Both mutations are nonsynonymous for M2 and result in the replacement of proline at position 10 by histidine (named P10H) or leucine (P10L), respectively (Fig. 5). Note that both mutations are synonymous for M1. Some isolates appeared to contain mainly mutant or wt sequences, whereas

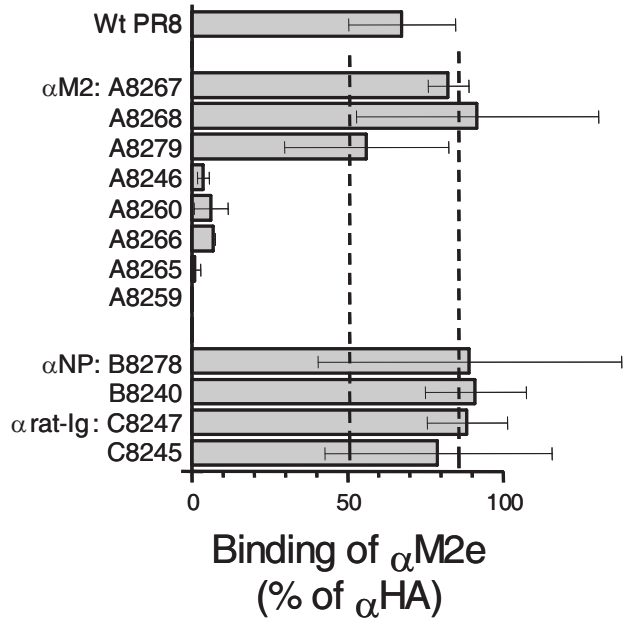

FIG. 4. Antigenic analysis of virus isolates. Replicate MDCK cell monolayers in 96-well plates were infected with egg-grown lung virus isolates derived from mice treated with the M2e-specific MAb 14C2-S1-4 (isolate notation A) or with NP-specific (B isolates) or rat immunoglobulin-specific (C isolates) control MAbs. The virus isolates used for infection of the MDCK cells are indicated to the left of each bar. They were obtained from severely moribund mice (>30% weight loss) or at termination of experiments, ranging from days 33 to 46 (isolates A) and days 16 to 34 (isolates B and C). PR8 wt is the virus used for infection of the mice. After 8 h of incubation at 37°C, infected monolayers were fixed with formalin and tested by ELISA for reaction with the HA-specific MAb H36-4 and the M2e-specific MAb 14C2, both at 1 μg/ml, in three replicates per MAb. For each isolate, the average OD (above background) seen with the M2e-specific MAb was expressed as percentage of the OD seen with HA-specific MAb. Assay background was determined with the nonreactive MAb 14-4-4S. Each bar shows the mean percent ± 95% confidence interval of at least three assays performed with MDCK cell monolayers infected with different doses of virus isolate. The stipulated vertical lines show the 95% confidence interval seen with MDCK cell monolayers infected with wt PR8 virus.

others clearly contained mixtures of mutant and wt sequences (Fig. 5). None of the isolates revealed the concomitant presence of two escape mutants. Overall, M2e mutants were observed in 22 of 34 (65%) lung isolates from mice treated with anti-M2e MAbs but in none of 11 lung isolates from mice treated with control (anti-NP or anti-rat Cκ) MAbs. This difference is highly significant (χ^2, $P < 0.001$) and indicates that the presence of M2e-specific MAbs provided a selective environment for the outgrowth of these virus mutants. P10H and P10L mutants arose at similar frequency in 13 and 9 mice, respectively. P10H mutants emerged also in five of five anti-M2e-MAb-treated SCID mice that were infected with X31, a reassortant virus that differs from PR8 by expression of H3 and N2 glycoproteins and lower pathogenicity (data not shown).

Biologic properties of the M2e mutants. The above findings indicated that PR8 was capable of escaping anti-M2e MAb-mediated growth restriction by mutation(s). To investigate the antigenic and biologic consequences of these mutations in more detail, P10H and P10L from two lung isolates were cloned by limiting dilution in MDCK cell microcultures and expanded by growth in the allantoic cavity of embryonated hen's eggs. As a control, a lung isolate from an anti-M2e MAb-treated mouse without mutation in M2e (P10) was similarly cloned. The cloned viruses were then compared to wt PR8 for recognition by M2e-specific MAbs and antisera, growth in vitro, pathogenicity, and susceptibility to anti-M2e MAb-mediated growth restriction in vivo.

Egg-grown P10L, P10H, and P10 isolates showed similar infectivity for MDCK cells ($10^{5.9}$ to $10^{6.1}$ $TCID_{50}$/HAU) and replicated at similar rate in MDCK cell cultures in vitro as wt PR8 (Fig. 6A). None of the available MAbs specific for wt M2e cross-reacted with the escape mutants (Fig. 6C), and sera from mice immunized with M2e-MAP (21) showed 10- to 100-fold reduced binding to P10H and P10L, respectively, compared to P10 (Fig. 6B). Thus, P10H and P10L appeared to display major antigenic alterations in relation to this panel of wt M2e-specific MAbs and antisera.

To test whether the escape mutations altered viral pathogenicity, we compared the isolates for induction of disease and mortality in BALB/c mice. We used in this case an inoculum of 50 μl, which initiates infection throughout the entire respiratory tract and represents a more severe challenge than the infection that is initially confined to the nasal epithelium. Mice infected with 500 or 1,500 $TCID_{50}$ of P10H and P10 showed lesser morbidity (Fig. 7A and B) and mortality (Fig. 7C and D) than mice infected with the same doses of wt PR8. In contrast, P10L retained the high pathogenicity of wt PR8. The finding that the P10 isolate differed in pathogenicity from wt PR8 suggests that it, and probably also the escape mutants P10H and P10L, had acquired additional unknown mutations in the course of the many rounds of replication in vivo.

Finally, to confirm that the P10H and P10L isolates indeed were functional escape mutants, we tested them for the ability to induce disease in SCID mice in the presence of passive M2e-specific MAb. As shown in Fig. 8C and D, MAb M2-56 lacked protective activity against P10H and P10L but, as expected, delayed disease in mice infected with wt PR8 (Fig. 8A). The isolate with nonmutated M2e (P10) remained susceptible to the protective activity of M2-56 (Fig. 8B), indicating that it had not acquired mutation(s) that may have rendered it resistant to anti-M2e Ab-mediated protection in vivo, as has been observed previously in an in vitro model (1).

DISCUSSION

The interest in M2e as a vaccine target is based on two premises: (i) the remarkably high structural conservation of this protein region among human epidemic influenza type A virus strains and (ii) evidence obtained from various animal models indicating that M2e-specific immunity can significantly decrease morbidity and mortality associated with influenza virus infection. The finding that PR8 could escape anti-M2e Ab-mediated protection in vivo by acquisition of mutations may raise concerns regarding the usefulness of M2e as a highly conserved vaccine target, and several aspects of this observation merit further discussion.

First, although virus mutants emerged in 65% of the anti-M2e Ab-treated mice, they were of highly restricted diversity since only two distinct mutants were observed repetitively in many individual mice, one with a proline-to-histidine inter-

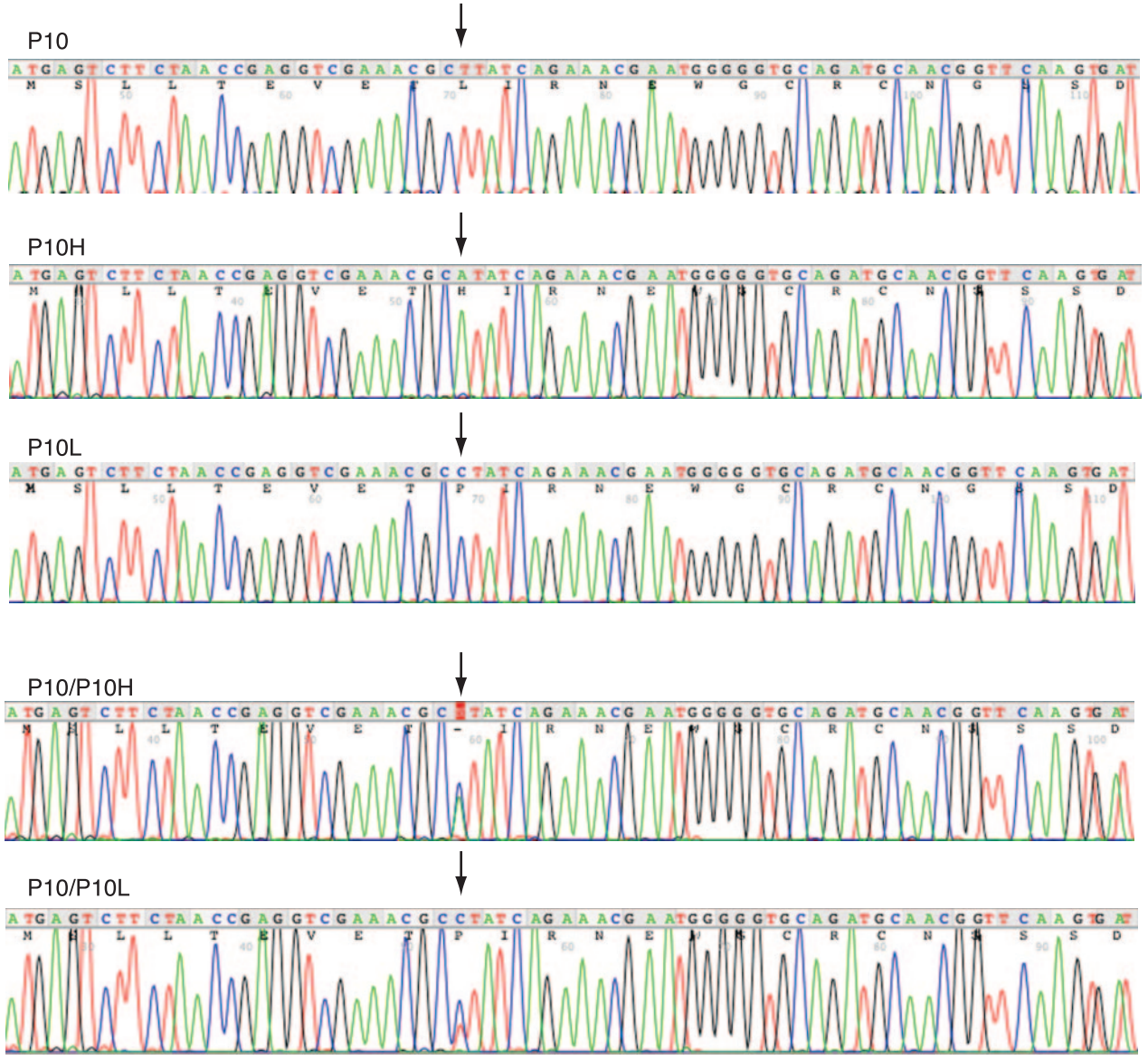

FIG. 5. Sequence analysis of virus isolates. Sequence chromatograms of the M2e region were generated directly from M2 PCR products by using the sequence primer M2-1 Rev (see Materials and Methods). Corresponding nucleotide and protein sequences are shown above each chromatogram. The arrow indicates nucleotide position 29 (amino acid position 10 of M2e). The three top chromatograms exemplify isolates that appeared to contain only wt virus and the P10H and P10L mutants, respectively. The bottom two chromatograms exemplify isolates that contained mixtures of wt and a mutant virus.

change at amino acid position 10 (P10H) and the other with a proline-to-leucine (P10L) interchange at the same position. A trivial explanation for the repetitive isolation of only two mutants would be their existence at high frequency (~1 per 10^4 $TCID_{50}$) in the wt PR8 virus preparation. This possibility can be excluded because it would have resulted in the relatively frequent isolation of both mutants from individual mice, which was not the case. In addition, if the mutants had been introduced into the mice at the time of infection, Ab treatment could not have prolonged survival by more than 1 day, i.e., the time required for the infecting mutant virus to generate ~10^4 progeny viruses. Therefore, these escape mutants must have arisen during replication of the wt PR8 virus in vivo. Furthermore, in view of the isolation of only two distinct mutants, it is important to note that typical Ab binding sites make contact with 13 to 17 amino acid residues of their corresponding epitopes (1, 2, 5, 8), and changes at many of these would likely have resulted in strongly decreased binding of the Ab to the altered epitope. For instance, viral escape mutants selected in the presence of individual HA-specific MAbs exhibited single point mutations at four to five different residues (2, 4), even though the selection experiments were much less exhaustive than the ones performed here. Thus, since mutations arise randomly in the course of viral gene transcription, the finding that only two distinct mutants emerged implies a strong constraint against most changes within the epitopes defined by the

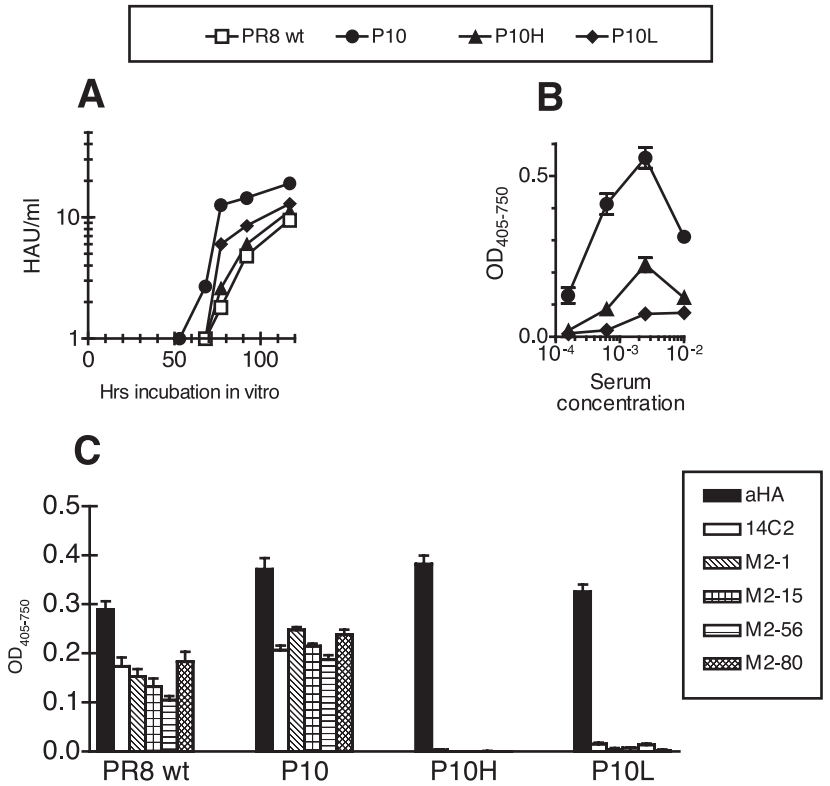

FIG. 6. Growth kinetics of mutants in MDCK cells in vitro and their antigenicity. (A) Six replicate MDCK cell microcultures were infected with wt PR8, P10, P10L, or P10H and then cultured for 5 days. Small samples a culture medium were harvested at 10- to 14-h intervals and pooled within replicate cultures. The samples were then tested for virus titer by HA test. The figure shows the results of a representative experiment in which the cells were infected with 10 $TCID_{50}$ of virus. (B) A pool of sera obtained from four BALB/c mice 2 weeks after the third i.n. inoculation with 5 μg of wt M2e-MAP, together with 3 μg of immunostimulatory ODN and 0.5 μg of cholera toxin as described previously (21), was tested in an ELISA for reaction with MDCK cell monolayers infected with the isolates P10, P10H, P10L, or B/Lee. ODs above B/Lee background (means and standard error of the mean [SEM] of triplicates) are shown. Similar results were obtained with sera from three other immunization experiments. (C) MDCK cell monolayers infected with the indicated viruses were tested in ELISA for recognition by purified HA- and M2e-specific MAbs. All MAbs were used at a saturating dose of 1 to 2 μg/ml. The columns show the mean ± the SEM of triplicates.

M2e-specific MAbs used here. As mentioned in the introduction, this is most likely because the gene segment that encodes M2e is bicistronic and encodes also parts of M1, the most conserved viral protein (13, 15). It is noteworthy that the P10L and P10H mutations are both synonymous for M1, i.e., do not result in a residue change in it.

In 35% of the anti-M2e Ab-treated mice we found no antigenic escape mutants, at least not at a frequency resulting in significant heterogeneity in the sequence chromatograms (Fig. 5). This is surprising in view of the reported mutation rate of 1.5×10^{-5}/bp/division of the influenza virus RNA genome (26). Thus, given the viral genome size of 13,600 nt, on average, one of five viral genomes would be expected to possess a point mutation and, assuming an equal mutation rate across the entire viral genome, one per 2×10^5 viral genomes would be expected to possess a defined nucleotide change at a given position such as the P10H or P10L mutations. Since this number of viral genomes would most likely be generated already during the first round of virus replication after infection with 10^4 $TCID_{50}$ of PR8, it is peculiar that no mutants were detected in 35% of the mice after several weeks of infection. The most likely explanation is that the emerging mutants were not single point mutants but required additional mutations, apart from the antigenic change in M2e, to become effective escape mutants. A requirement for additional specific mutations would decrease their frequency and increase the number of replication cycles needed for their selection. It is noteworthy that nine mutations were found in 10,641 M1-encoding nucleotides of M2e-escape mutants (data not shown). Six of these were synonymous and three nonsynonymous (A127T and V228L twice). The high frequency of nonselectable synonymous mutations is consistent with the notion that the selection of functional escape mutants occurred over many rounds of virus replication in vivo. Whether one or both of the two replacement mutations in M1 were selected or are nonrelevant mutations, carried along in the course of the selection process of the escape mutants, is unknown, but the latter appears more likely in view of the infrequent occurrence of these mutations. The absence of escape mutants in 35% of the anti-M2e MAb-treated SCID mice is also a reflection of the limited protective potency of M2e-specific MAbs, which can delay but not entirely prevent the spread of virus with nonmutated M2e.

Zebedee and Lamb (32) previously studied escape mutants that arose from influenza virus A/Udorn/72 in vitro in the presence of the anti-M2e MAb 14C2. A/Udorn, like most influenza type A viruses except for few strains such as PR8 and

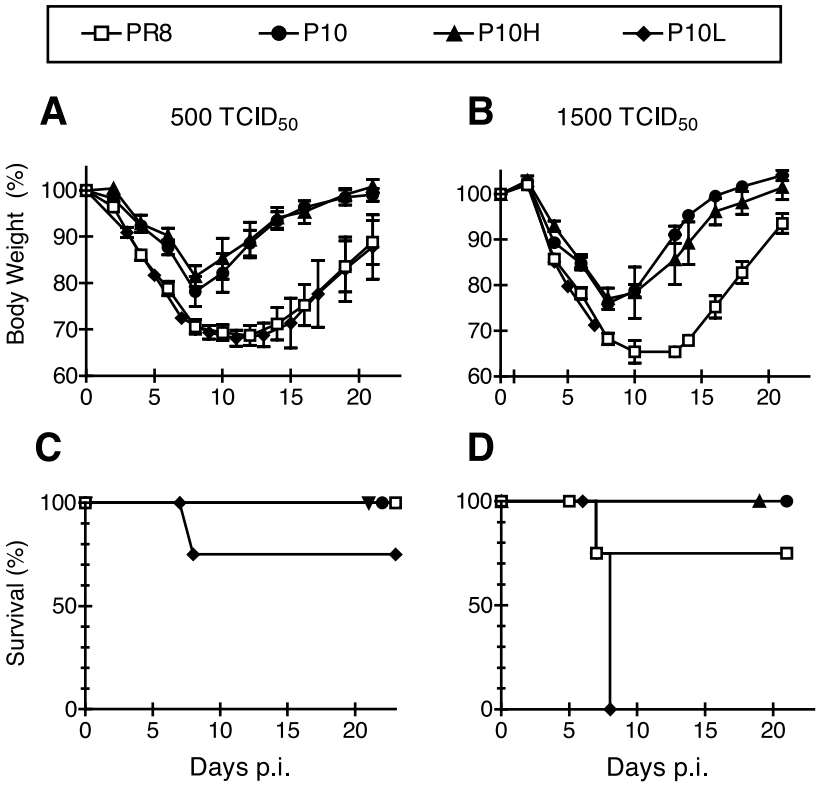

FIG. 7. Pathogenicity of M2e escape mutants in BALB/c mice. BALB/c mice (three to four/group) were infected i.n. with 500 $TCID_{50}$ (A and C) or 1,500 $TCID_{50}$ (B and D) of wt PR8 (□), P10 isolate (●), P10H (●), or P10L (◆). Infection was done under anesthesia with 50 μl of inoculum, which initiates a total respiratory tract infection. Mice were then observed for weight loss (A and B) and mortality (C and D). Panels A and C show the mean ± the SEM within each group. Since BALB/c mice generate an immune response and may recover after loss of ≥30% of body weight, natural disease-associated death was used as the endpoint in panels C and D.

WSN/33 (33), is inhibited in its replication in vitro by MAb 14C2. Among the virus mutants that escaped this Ab-mediated growth restriction, only one was an antigenic mutant; it had an interchange of glutamic acid at position 8 by glycine (E8G). All other mutants were nonantigenic, i.e., contained the wt M2e but possessed mutations at positions 31 or 41 of M1 and positions 71 or 78 of M2. Although these nonantigenic escape mutants were still recognized by MAb 14C2, they were no longer inhibited in their growth in vitro by the MAb. We tested an isolate without M2e alteration (P10), which was derived from an anti-M2e MAb-treated mouse, for susceptibility to growth-restriction in vivo by anti-M2e Ab and found that it still was inhibited by MAb in vivo (Fig. 8B). Interestingly, the P10 isolate was less pathogenic than wt PR8 virus (Fig. 7), indicating that it had acquired one or several mutations that reduced its pathogenicity but not its susceptibility to Ab-mediated growth restriction in vivo. It is interesting also that the antigenic E8G mutation observed by Zebedee and Lamb (32) did not occur among the PR8 M2e-escape mutants. As argued above, the E8G mutation might have necessitated too many additional "compensatory" mutations on the PR8 background to make its emergence likely.

Both P10H and P10L replacements are found among the recent H5N1 and H7N7 isolates (Fig. 1B), which are believed to be direct transmissions of avian strains to humans, but have not occurred among transmissible human epidemic strains (Fig. 1A). Apparently, neither of these mutations seems to provide epidemic influenza virus strains with a growth advantage in humans. This could be because M2e-specific Abs, if present, do not restrict virus growth in humans, as reported recently for pigs (10). More likely, the absence of these mutations among human epidemic strains is a reflection of the poor M2e-specific Ab response in humans, as indicated by two previous studies (3, 18). Further analyses of the M2e-specific Ab response in humans are likely to provide more insight into this important issue.

The finding that four distinct MAbs selected the same types of escape mutants shows that they delineate overlapping epitopes. This is not too surprising in view of the small size of M2e. In fact, the epitopes recognized by these MAbs is contained within the N-terminal 15 amino acids of M2e (unpublished observation), which is in agreement with a recent study reporting that two protective M2e-specific MAbs generated from BALB/c mice after immunization with a M2e-GST fusion protein were specific for a peptide corresponding to amino acids 6 to 13 of M2e (19). Thus, the size of the M2e antigenic determinant appears to be in the middle to low range of a typical protein epitope as revealed by X-ray crystallography of antigen-MAb complexes (1, 2, 5, 8). This may result in an oligoclonal anti-M2e Ab response and explain why it is of low titer after infection and typically becomes detectable only after a booster inoculation (21; unpublished observations). The oli-

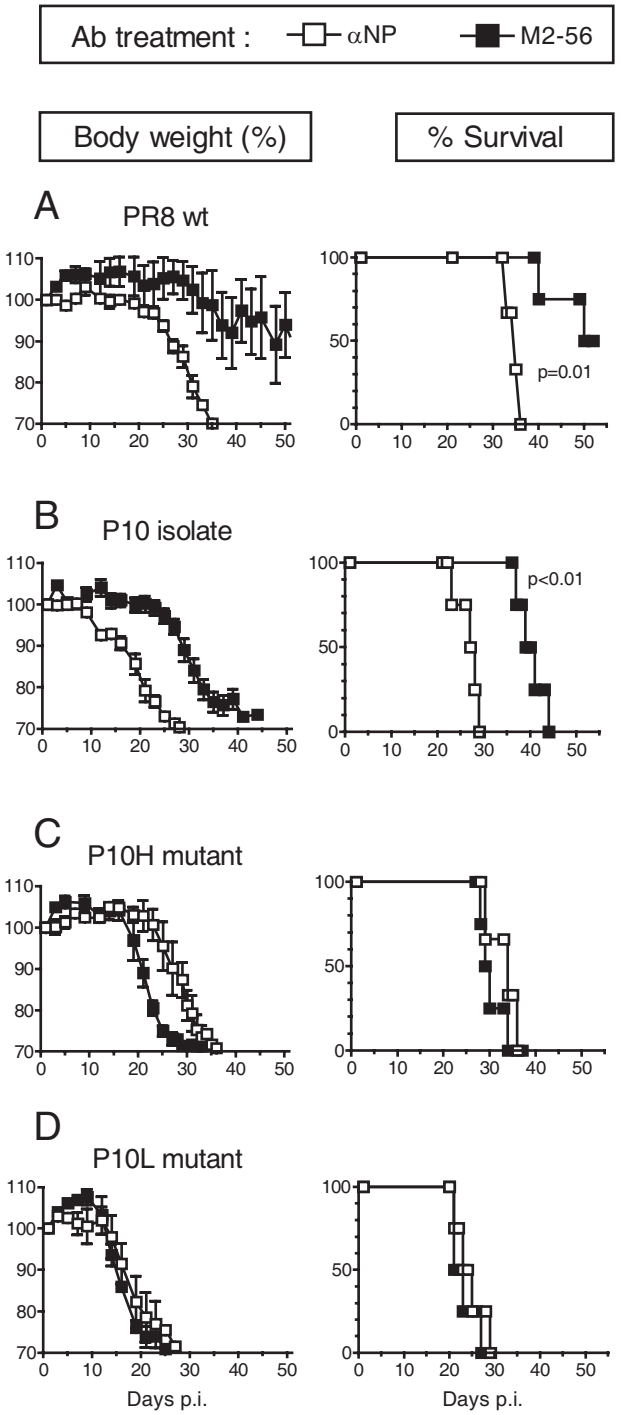

FIG. 8. P10H and P10L isolates are effective escape mutants. SCID mice (three to four per group) were infected i.n. with 5 μl (10^4 $TCID_{50}$) of PR8 (A), P10 (B), P10H (C), or P10L (D) and chronically treated with anti-NP MAb (open symbols) or anti-M2e MAb M2-56 (closed symbols) as described in the legend of Fig. 3. The mice were observed for body weight (panels on left) and survival (panels on right). The weight curves show the mean ± the SEM of the group. Mice were euthanized when their weight dropped below 70% of their initial body weight and this time point was taken as time of death. The statistical differences between survival curves were determined by log rank test and are indicated.

goclonality of this response in the BALB/c mouse is supported by the finding that all seven M2e-specific hybridomas, in spite of being isolated from three distinct donor mice, express the same heavy and one of two distinct light chain V genes and that hybridomas isolated from individual donor mice are clonally related (unpublished observation).

In conclusion, the results of the present study confirm the protective activity of M2e-specific Abs in vivo. However, compared to HA-specific Abs, which are capable of providing sterilizing immunity or resolving an established infection in SCID mice, M2e-specific protection is of lower potency and can decrease but not prevent or resolve infection. Thus, M2e will not be a substitute for the currently licensed vaccines that can induce much stronger protection if a reasonably good match exists between the vaccine and epidemic strain. Rather, M2e could be used as an adjunct to current vaccines and provide a protective safety net in the case of a major antigenic disparity between vaccine and circulating epidemic strains. The fact that M2e escape mutants arose in vivo in the presence of passive M2e-specific immunity does not preclude the use of M2e as a generic vaccine against influenza type A viruses as long as the structural variation remains small and all major variants can be incorporated into a "polyvalent" M2e vaccine. Based on the results from the present study, M2e remains a promising vaccine candidate for increasing the level of resistance against influenza type A virus infection in humans.

ACKNOWLEDGMENTS

This study was supported by NIH grants AI46457 and AI13989 and by the Commonwealth Universal Research Enhancement Program, Pennsylvania Department of Health.

The authors have no financial conflicts of interest.

We thank MeiFang Xie from the Genomic/Microarray core facility of the Wistar Institute for running the sequencer and William Wunner, Michael Showe, and Dimitri Negorev for reviewing the manuscript.

REFERENCES

1. **Amit, A. G., R. A. Mariuzza, S. E. Phillips, and R. J. Poljak.** 1986. Three-dimensional structure of an antigen-antibody complex at 2.8 Å resolution. Science **233:**747–753.
2. **Bizebard, T., B. Gigant, P. Rigolet, B. Rasmussen, O. Diat, P. Bosecke, S. A. Wharton, J. J. Skehel, and M. Knossow.** 1995. Structure of influenza virus haemagglutinin complexed with a neutralizing antibody. Nature **376:**92–94.
3. **Black, R. A., P. A. Rota, N. Gorodkova, H. D. Klenk, and A. P. Kendal.** 1993. Antibody response to the M2 protein of influenza A virus expressed in insect cells. J. Gen. Virol. **74**(Pt. 1)**:**143–146.
4. **Caton, A. J., G. G. Brownlee, J. W. Yewdell, and W. Gerhard.** 1982. The antigenic structure of the influenza virus A/PR/8/34 hemagglutinin (H1 subtype). Cell **31:**417–427.
5. **Colman, P. M., W. G. Laver, J. N. Varghese, A. T. Baker, P. A. Tulloch, G. M. Air, and R. G. Webster.** 1987. Three-dimensional structure of a complex of antibody with influenza virus neuraminidase. Nature **326:**358–363.
6. **Fan, J., X. Liang, M. S. Horton, H. C. Perry, M. P. Citron, G. J. Heidecker, T. M. Fu, J. Joyce, C. T. Przysiecki, P. M. Keller, V. M. Garsky, R. Ionescu, Y. Rippeon, L. Shi, M. A. Chastain, J. H. Condra, M. E. Davies, J. Liao, E. A. Emini, and J. W. Shiver.** 2004. Preclinical study of influenza virus A M2 peptide conjugate vaccines in mice, ferrets, and rhesus monkeys. Vaccine **22:** 2993–3003.
7. **Feng, J. Q., K. Mozdzanowska, and W. Gerhard.** 2002. Complement component C1q enhances the biological activity of influenza virus hemagglutinin-specific antibodies depending on their fine antigen specificity and heavy-chain isotype. J. Virol. **76:**1369–1378.
8. **Fleury, D., B. Barrere, T. Bizebard, R. S. Daniels, J. J. Skehel, and M. Knossow.** 1999. A complex of influenza hemagglutinin with a neutralizing antibody that binds outside the virus receptor binding site. Nat. Struct. Biol. **6:**530–534.
9. **Frace, A. M., A. I. Klimov, T. Rowe, R. A. Black, and J. M. Katz.** 1999. Modified M2 proteins produce heterotypic immunity against influenza A virus. Vaccine **17:**2237–2244.
10. **Heinen, P. P., F. A. Rijsewijk, E. A. de Boer-Luijtze, and A. T. Bianchi.** 2002.

Vaccination of pigs with a DNA construct expressing an influenza virus M2-nucleoprotein fusion protein exacerbates disease after challenge with influenza A virus. J. Gen. Virol. **83:**1851–1859.
11. **Hoffmann, E., J. Stech, Y. Guan, R. G. Webster, and D. R. Perez.** 2001. Universal primer set for the full-length amplification of all influenza A viruses. Arch. Virol. **146:**2275–2289.
12. **Holsinger, L. J., and R. A. Lamb.** 1991. Influenza virus M2 integral membrane protein is a homotetramer stabilized by formation of disulfide bonds. Virology **183:**32–43.
13. **Ito, T., O. T. Gorman, Y. Kawaoka, W. J. Bean, and R. G. Webster.** 1991. Evolutionary analysis of the influenza A virus M gene with comparison of the M1 and M2 proteins. J. Virol. **65:**5491–5498.
14. **Jegerlehner, A., N. Schmitz, T. Storni, and M. F. Bachmann.** 2004. Influenza A vaccine based on the extracellular domain of M2: weak protection mediated via antibody-dependent NK cell activity. J. Immunol. **172:**5598–5605.
15. **Lamb, R. A., C. J. Lai, and P. W. Choppin.** 1981. Sequences of mRNAs derived from genome RNA segment 7 of influenza virus: colinear and interrupted mRNAs code for overlapping proteins. Proc. Natl. Acad. Sci. USA **78:**4170–4174.
16. **Lamb, R. A., S. L. Zebedee, and C. D. Richardson.** 1985. Influenza virus M2 protein is an integral membrane protein expressed on the infected-cell surface. Cell **40:**627–633.
17. **Liang, S., K. Mozdzanowska, G. Palladino, and W. Gerhard.** 1994. Heterosubtypic immunity to influenza type A virus in mice. Effector mechanisms and their longevity. J. Immunol. **152:**1653–1661.
18. **Liu, W., H. Li, and Y. H. Chen.** 2003. N terminus of M2 protein could induce antibodies with inhibitory activity against influenza virus replication. FEMS Immunol. Med. Microbiol. **35:**141–146.
19. **Liu, W., P. Zou, and Y. H. Chen.** 2004. Monoclonal antibodies recognizing EVETPIRN epitope of influenza A virus M2 protein could protect mice from lethal influenza A virus challenge. Immunol. Lett. **93:**131–136.
20. **Macken, C., H. Lu, J. Goodman, and L. Boykin.** 2001. The value of a database in surveillance and vaccine selection, p. 103–106. *In* A. D. M. E. Osterhaus, N. J. Cox, and A. W. Hampson (ed.), Options for the control of influenza. Elsevier Science, Amsterdam, The Netherlands.
21. **Mozdzanowska, K., J. Feng, M. Eid, G. Kragol, M. Cudic, L. Otvos, Jr., and W. Gerhard.** 2003. Induction of influenza type A virus-specific resistance by immunization of mice with a synthetic multiple antigenic peptide vaccine that contains ectodomains of matrix protein 2. Vaccine **21:**2616–2626.
22. **Mozdzanowska, K., J. Feng, and W. Gerhard.** 2003. Virus-neutralizing activity mediated by the Fab fragment of a hemagglutinin-specific antibody is sufficient for the resolution of influenza virus infection in SCID mice. J. Virol. **77:**8322–8328.
23. **Mozdzanowska, K., K. Maiese, M. Furchner, and W. Gerhard.** 1999. Treatment of influenza virus-infected SCID mice with nonneutralizing antibodies specific for the transmembrane proteins matrix 2 and neuraminidase reduces the pulmonary virus titer but fails to clear the infection. Virology **254:** 138–146.
24. **Neirynck, S., T. Deroo, X. Saelens, P. Vanlandschoot, W. M. Jou, and W. Fiers.** 1999. A universal influenza A vaccine based on the extracellular domain of the M2 protein. Nat. Med. **5:**1157–1163.
25. **Palladino, G., K. Mozdzanowska, G. Washko, and W. Gerhard.** 1995. Virus-neutralizing antibodies of immunoglobulin G (IgG) but not of IgM or IgA isotypes can cure influenza virus pneumonia in SCID mice. J. Virol. **69:** 2075–2081.
26. **Parvin, J. D., A. Moscona, W. T. Pan, J. M. Leider, and P. Palese.** 1986. Measurement of the mutation rates of animal viruses: influenza A virus and poliovirus type 1. J. Virol. **59:**377–383.
27. **Pinto, L. H., L. J. Holsinger, and R. A. Lamb.** 1992. Influenza virus M2 protein has ion channel activity. Cell **69:**517–528.
28. **Slepushkin, V. A., J. M. Katz, R. A. Black, W. C. Gamble, P. A. Rota, and N. J. Cox.** 1995. Protection of mice against influenza A virus challenge by vaccination with baculovirus-expressed M2 protein. Vaccine **13:**1399–1402.
29. **Sugrue, R. J., and A. J. Hay.** 1991. Structural characteristics of the M2 protein of influenza A viruses: evidence that it forms a tetrameric channel. Virology **180:**617–624.
30. **Takeda, M., G. P. Leser, C. J. Russell, and R. A. Lamb.** 2003. Influenza virus hemagglutinin concentrates in lipid raft microdomains for efficient viral fusion. Proc. Natl. Acad. Sci. USA **100:**14610–14617.
31. **Treanor, J. J., E. L. Tierney, S. L. Zebedee, R. A. Lamb, and B. R. Murphy.** 1990. Passively transferred monoclonal antibody to the M2 protein inhibits influenza A virus replication in mice. J. Virol. **64:**1375–1377.
32. **Zebedee, S. L., and R. A. Lamb.** 1989. Growth restriction of influenza A virus by M2 protein antibody is genetically linked to the M1 protein. Proc. Natl. Acad. Sci. USA **86:**1061–1065.
33. **Zebedee, S. L., and R. A. Lamb.** 1988. Influenza A virus M2 protein: monoclonal antibody restriction of virus growth and detection of M2 in virions. J. Virol. **62:**2762–2772.